Antimony in Mount Bonnie and Iron Blow mine wastes, Northern Territory

Allan S Gomes[1,2], *Kamini Bhowany*[1], *Laura Jackson*[1] *and Anita Parbhakar-Fox*[1]

Introduction

Antimony is a chalcophile element that often occurs as stibnite (Sb_2S_3), sulphosalts (eg tetrahedrite – $Cu_6[Cu_4(Fe,Zn)_2]Sb_4S_{13}$) and oxides (eg valentinite – Sb_2O_3); it is commonly associated with gold mineralisation and polymetallic silver–lead–zinc deposits (Filella *et al* 2002, Schwarz-Schampera 2014, Britt and Senior 2021, Radková *et al* 2023). Antimony has multiple applications across various industries due to its unique properties; its main uses are in fire retardants, lead-acid batteries, lead alloys, semiconductors, plastic catalysts, ceramics, and glass manufacturing (Schwarz-Schampera 2014, Radková *et al* 2023). Importantly, antimony features on the critical minerals list of multiple countries, such as Australia (Geoscience Australia 2024), Canada (Geological Survey of Canada 2023) and United States (U.S. Geological Survey 2024). By definition, critical minerals refer to metallic or non-metallic elements that are deemed essential for the economic and industrial well-being of a country, and the supply of which may be at risk due to potential geopolitical, economic, or supply chain disruptions (Geoscience Australia 2024). Geochemical and mineral characterisation research programs are therefore fundamental to determine critical metal tenor and mode of occurrence, as well as their potential for extraction (van der Ent *et al* 2021).

In addition to primary mineral deposits, antimony and other critical metals may be found in ore grade concentrations in mine wastes, such as tailings, waste rocks, and slags (Zhou *et al* 2017, Radková *et al* 2023). Increasing demand for critical metals therefore makes mine waste a potential target for mineral exploration (Dold 2020, van der Ent *et al* 2021). Moreover, the reuse and recycling of mine wastes constitute vital components within a comprehensive set of strategies to improve resource efficiency and mitigate the environmental impact of mining activities (van der Ent *et al* 2021). Examples of successful cases of effective mine waste recycling include the polymetallic Olympic Dam mine in South Australia, where copper and uranium are recovered from flotation tailings (Lèbre *et al* 2017); and Peko tailings dump in the Northern Territory, where cobalt is recovered from pyrite (McEwan and Ralph 2002).

Bulk-rock geochemistry analysis conducted during earlier phases of this research revealed that Mount Bonnie and Iron Blow mine wastes (**Figure 1**) are well-endowed with antimony, having concentrations up to 5110 ppm Sb in Mount Bonnie waste rocks and up to 4930 ppm Sb in Iron Blow waste rocks (**Figure 2**; Bhowany *et al* 2023, Gomes *et al* 2023). In this study, we provide further details on antimony deportment in Mount Bonnie and Iron Blow mine wastes.

[1] University of Queensland, Sustainable Minerals Institute, 40 Isles Rd, Indooroopilly QLD 4068, Australia
[2] Email: a.gomes@uq.edu.au

Background

The Pine Creek Orogen comprises a Palaeoproterozoic succession of metasedimentary (eg sandstones, shales, cherts, and carbonates) and volcaniclastic rocks intruded by syn- to post-tectonic granitoids and mafic bodies (Stuart-Smith *et al* 1993, Worden *et al* 2008, Raymond *et al* 2012, Ahmad and Hollis 2013). Importantly, the Pine Creek Orogen hosts multiple mineral commodities, such as gold, uranium and polymetallic nickel–cobalt–lead–copper deposits (Worden *et al* 2008, Ahmad and Hollis 2013). At Mount Bonnie and Iron Blow, gold deposits occur as lenses within interbedded pyritic shale, dolomitic siltstone and tuff within the Mount Bonnie Formation of the South Alligator Group (Ahmad and Hollis 2013).

Mine wastes from seven sites across the Northern Territory – mostly historical gold mines – were sampled between 2022 and 2023 as part of collaborative projects with the Northern Territory Geological Survey (NTGS) through the *Secondary Prospectivity of Mine Waste Project*, and with Geoscience Australia (GA) through the *Exploring for the Future* program (Bhowany *et al* 2023). Whole-rock geochemistry has indicated that Mount Bonnie and Iron Blow mine wastes are particularly endowed with critical metals such as arsenic, bismuth, molybdenum, antimony, selenium, and tellurium; precious and base metals such as silver, gold, cadmium, copper, lead, and zinc are also present in significant concentrations (Bhowany *et al* 2023, Gomes *et al* 2023). Mineralogical investigations through X-ray diffraction, mineral liberation analysis (MLA) and laser ablation inductively coupled plasma mass spectrometry (LA–ICP–MS) revealed iron oxide (goethite and hematite) as a potential host for antimony and other critical metals (**Figure 3**; Gomes *et al* 2023). Sample time (s) vs intensity (cps) plots also show that iron oxide has elevated antimony throughout the mineral matrix and is not associated with inclusions (**Figure 4**; Gomes *et al* 2023).

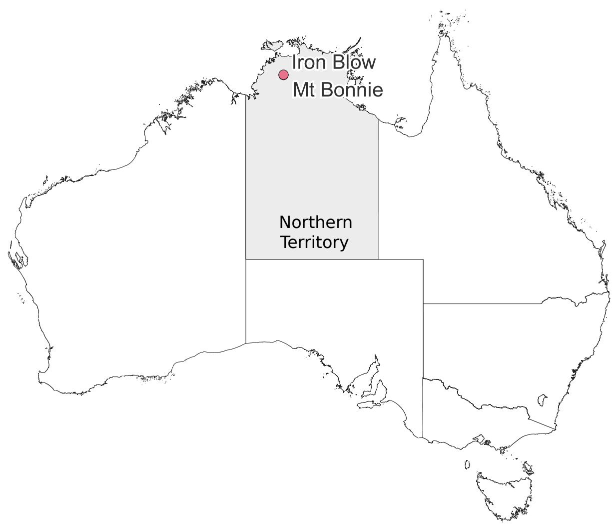

Figure 1. Location of Mount Bonnie and Iron Blow mining sites in the Northern Territory.

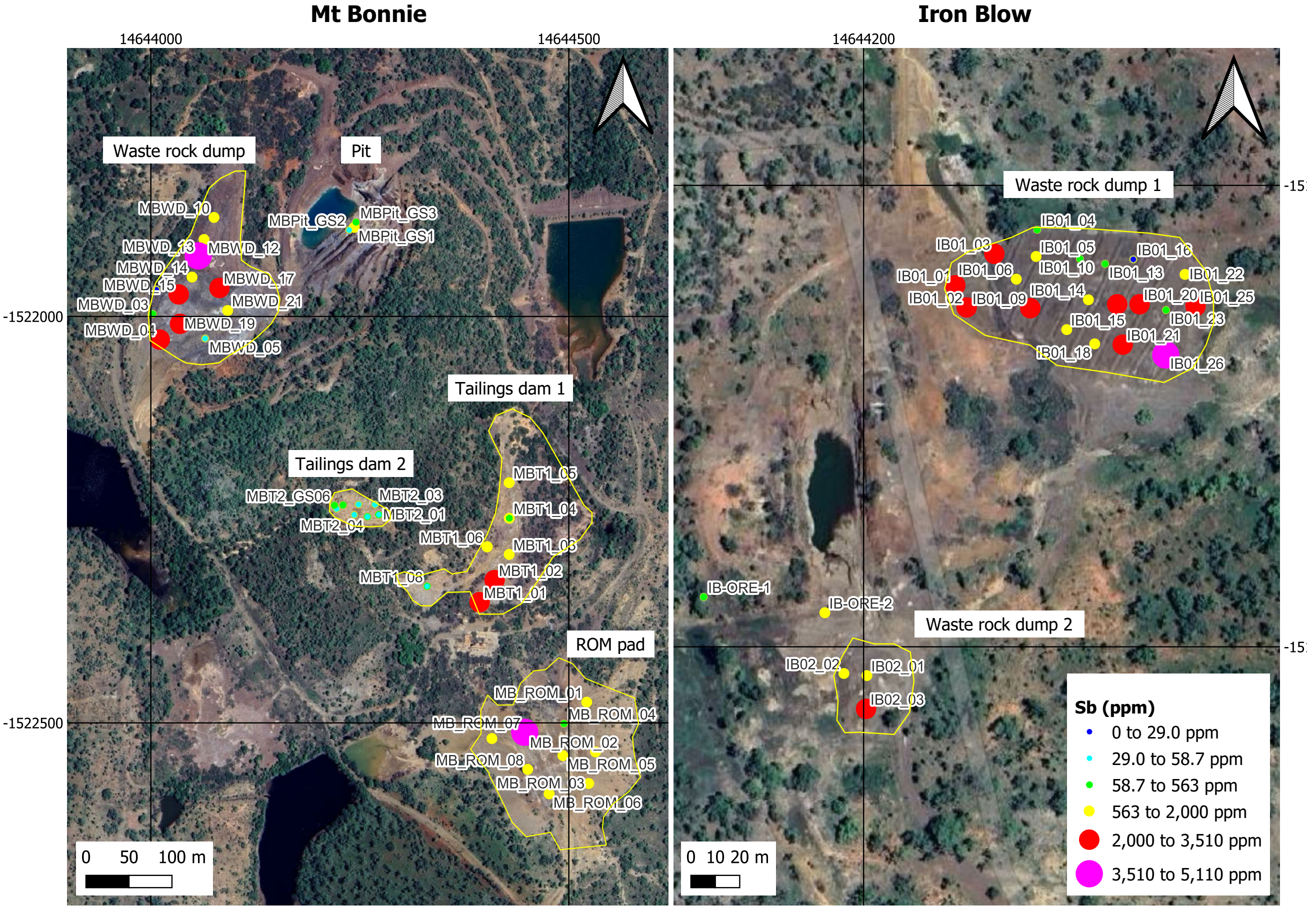

Figure 2. Spatial distribution of antimony (ppm) across Mount Bonnie (left) and Iron Blow (right).

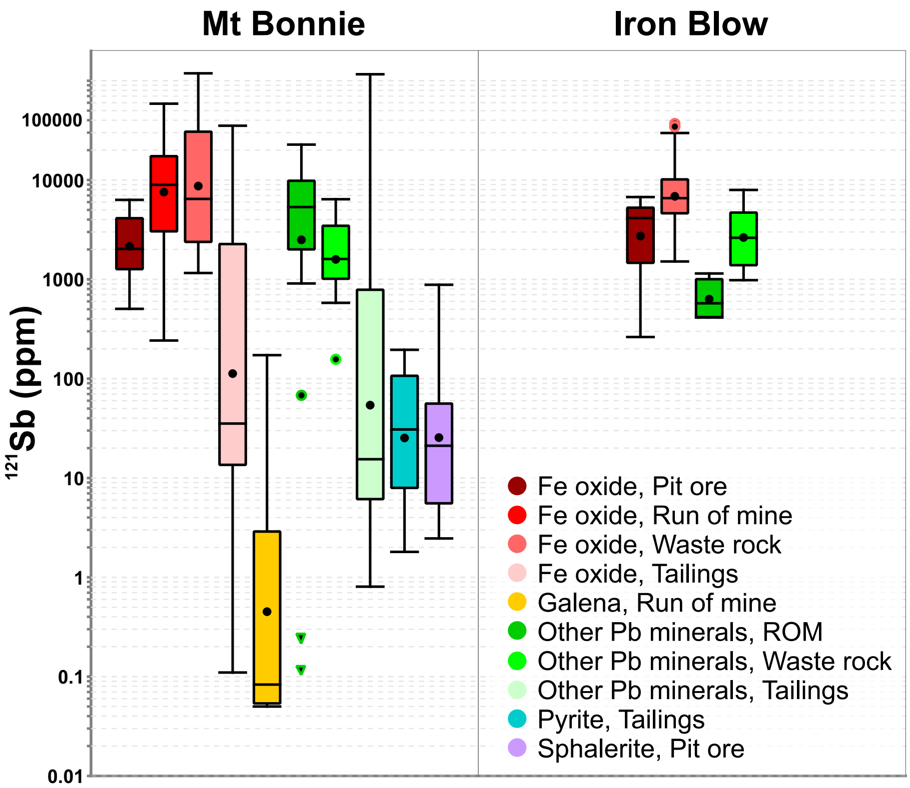

Figure 3. Antimony concentrations in Mount Bonnie and Iron Blow samples as determined by LA–ICP–MS.

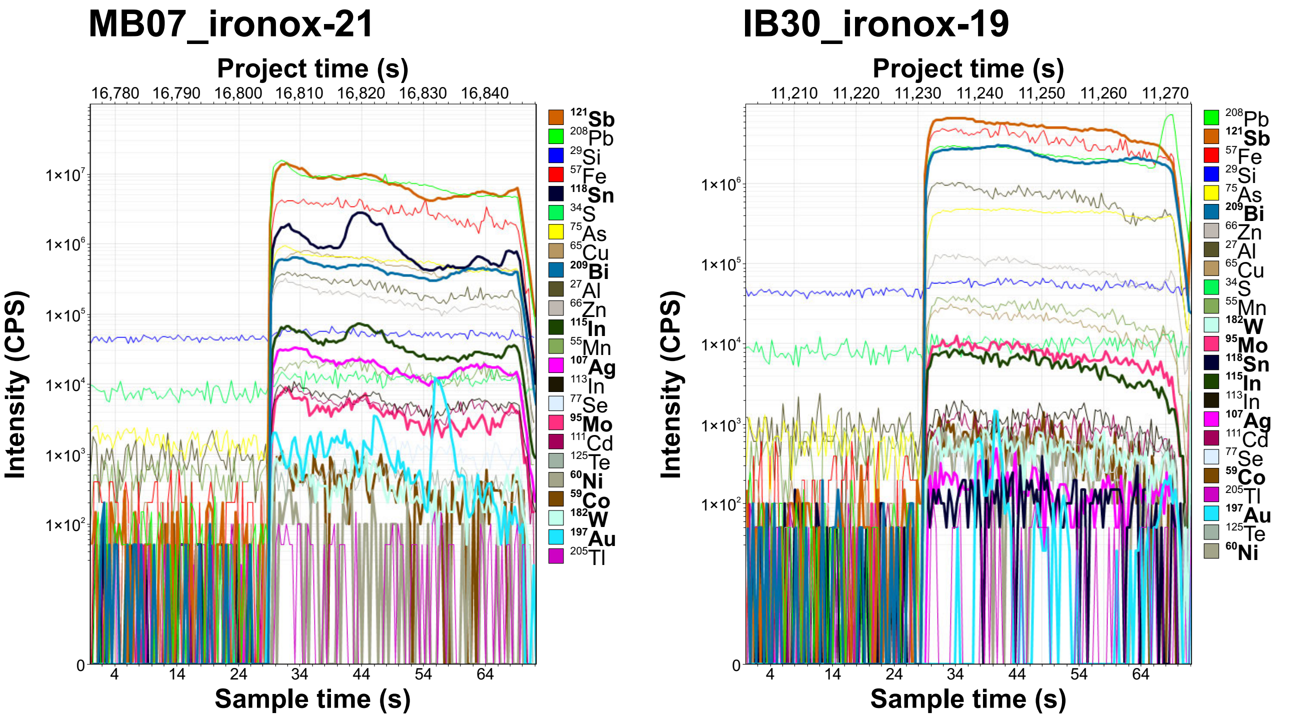

Figure 4. LA–ICP–MS pattern for Mount Bonnie ROM sample MB07_ironox-21 (58 740 ppm Sb) and Iron Blow waste rock sample IB30_ironox-19 (37 033 ppm Sb).

Methods

Waste rock samples endowed with antimony (IB30: Iron Blow waste rock, 4930 ppm Sb; MB11: Mount Bonnie run of mine, 3790 ppm Sb) were investigated in detail with a Hitachi TM3030 scanning electron microscope (SEM) coupled with a Bruker Quantax 70 energy dispersive x-ray spectrometer (EDS) at the Centre for Microscopy and Microanalysis of The University of Queensland (CMM/UQ). Prior to analysis, each mount was carbon-coated using a Quorum Q150T carbon coater. The SEM was operated using a 25 kV accelerating voltage, a 10 mm working distance and a 70 µm spot size. Whenever possible, EDS analysis was conducted alongside LA–ICP–MS spots for result comparison.

Preliminary results

Iron oxide occurs as goethite and hematite in the samples analysed and is found along with quartz and lead sulfates. Goethite and hematite were tentatively distinguished based on their different shades of grey on backscattered electron (BSE) images. They may be present as: 1) goethite/hematite aggregates, 2) radial-fibrous goethite crystals, 3) botryoidal goethite/hematite crystals, 4) fine-grained fibrous goethite/hematite aggregates, 5) 'vuggy' iron oxide crystals, and 6) antimony-rich iron oxide 'veins' (**Figure 5**).

Preliminary EDS results indicate that there are significant compositional differences between iron oxide forms (**Table 1**). Goethite/hematite aggregates, which appear to have been the first generation of iron oxides formed in sample IB-30 (**Figure 5A**), show the highest antimony concentrations (up to 16.6 wt% Sb) and therefore are the main targets for antimony investigation in that sample (**Figure 6**). Importantly, antimony seems to have been incorporated throughout the iron oxide matrix and is not associated with inclusions, which is consistent with LA–ICP–MS observations (**Figure 4**). All other forms of iron oxide in sample IB-30 (eg radial-fibrous goethite, botryoidal goethite/hematite, fine-grained goethite), which seem to have been formed following the first generation of iron oxides, are relatively poor in antimony (up to 1.2 wt% Sb) but often have higher lead, arsenic and zinc content.

Preliminary EDS results for sample MB-11 slightly differ from those of sample IB-30. The earliest goethite/hematite phases mostly have low antimony concentrations (**Figure 6**; **Table 2**), and antimony enrichment seems random. Late-stage radial-fibrous goethite is characterised by lower antimony and higher zinc (**Table 2**). However, other seemingly late-stage iron oxide phases (ie the 'vuggy' hematite and the antimony-rich iron oxide 'veins') yield the highest antimony concentrations in sample MB-11 (up to 24.9 wt% Sb in the antimony-rich iron oxide 'veins'). This indicates that antimony-bearing fluids were still actively percolating during different stages of iron oxide growth.

Next steps

Additional mineralogical investigations will be conducted through LA–ICP–MS mapping and electron microprobe to obtain refined compositional maps and more accurate and precise analytical results. This will help in characterising the mode of occurrence of antimony in Mount Bonnie and Iron Blow waste rocks.

Considering the economic and environmental benefits of recovering critical metals from mine waste, it is recommended to explore innovative extraction and separation techniques that can effectively recover

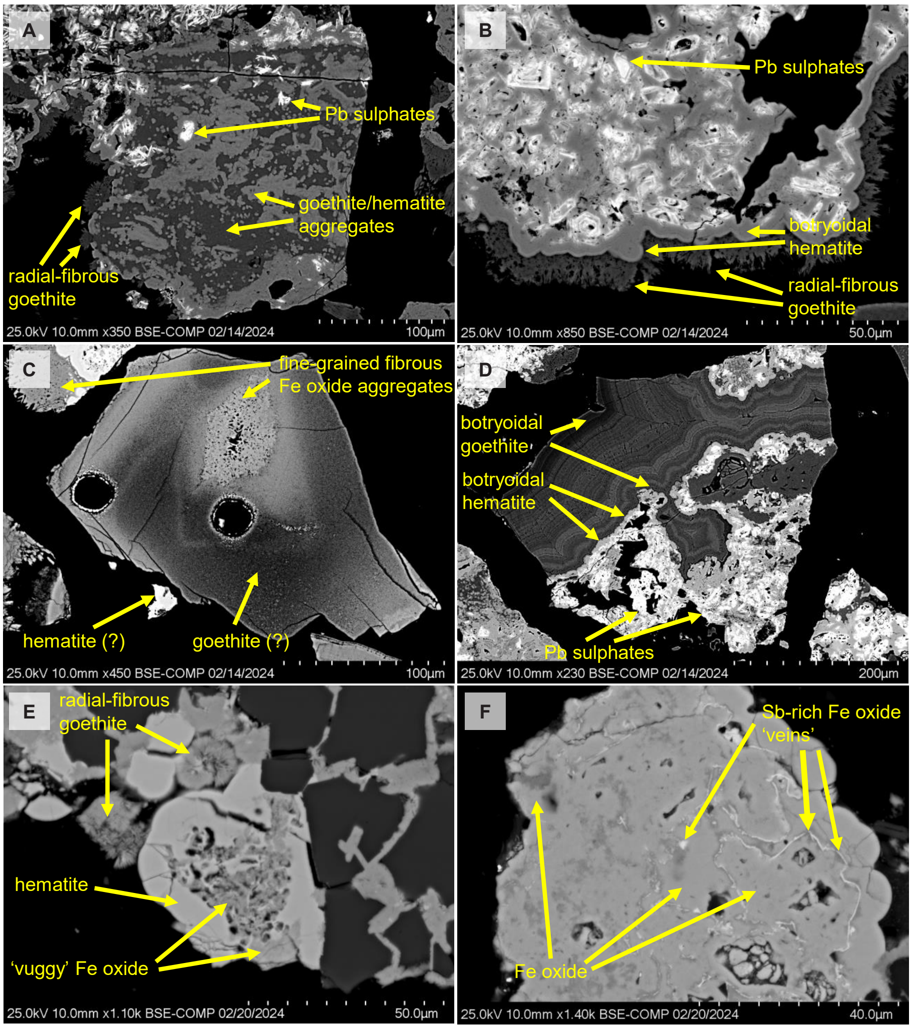

Figure 5. BSE images showing the different iron oxide modes of occurrence in samples IB-30 (A–D) and MB-11 (E–F).

Phase	Fe (wt%)	Sb (wt%)	Pb (wt%)	As (wt%)	Zn (wt%)
Fe oxide (goethite) (n = 28)					
min	76.4	0.6	0.5	0.4	0.2
max	95.4	16.6	4.3	1.3	3.4
average	89.6	**5.1**	1.5	0.9	0.7
median	91.2	3.8	1.4	0.9	0.4
Fe oxide (hematite) (n = 9)					
min	89.1	0.4	1.2	0.6	0.2
max	94.2	6.0	3.0	1.0	0.4
average	91.1	**4.1**	1.9	0.8	0.3
median	90.0	4.9	1.7	0.8	0.3
Fe oxide (radial-fibrous goethite) (n = 7)					
min	83.8	1.1	1.3	0.6	3.0
max	92.0	1.2	1.8	0.8	3.4
average	89.4	1.1	1.6	0.7	3.2
median	91.0	1.1	1.6	0.7	3.3
Fe oxide (fine-grained goethite) (n = 2)					
min	89.3	0.8	1.9	0.7	3.3
max	91.5	0.8	2.3	1.9	4.8
average	90.4	0.8	2.1	1.3	4.1
median	90.4	0.8	2.1	1.3	4.1
Fe oxide (botryoidal goethite) (n = 10)					
min	87.5	0.0	0.8	1.7	0.0
max	90.1	0.7	2.8	4.1	4.8
average	88.6	0.4	2.0	2.6	3.3
median	88.5	0.4	2.1	2.6	3.4
Fe oxide (botryoidal hematite) (n = 6)					
min	84.4	0.4	1.5	0.4	0.4
max	95.6	0.8	6.6	1.0	0.5
average	92.7	0.6	2.9	0.8	0.4
median	94.5	0.7	2.1	0.9	0.4

Table 1. Summary statistics of EDS results for iron oxide from sample IB-30.

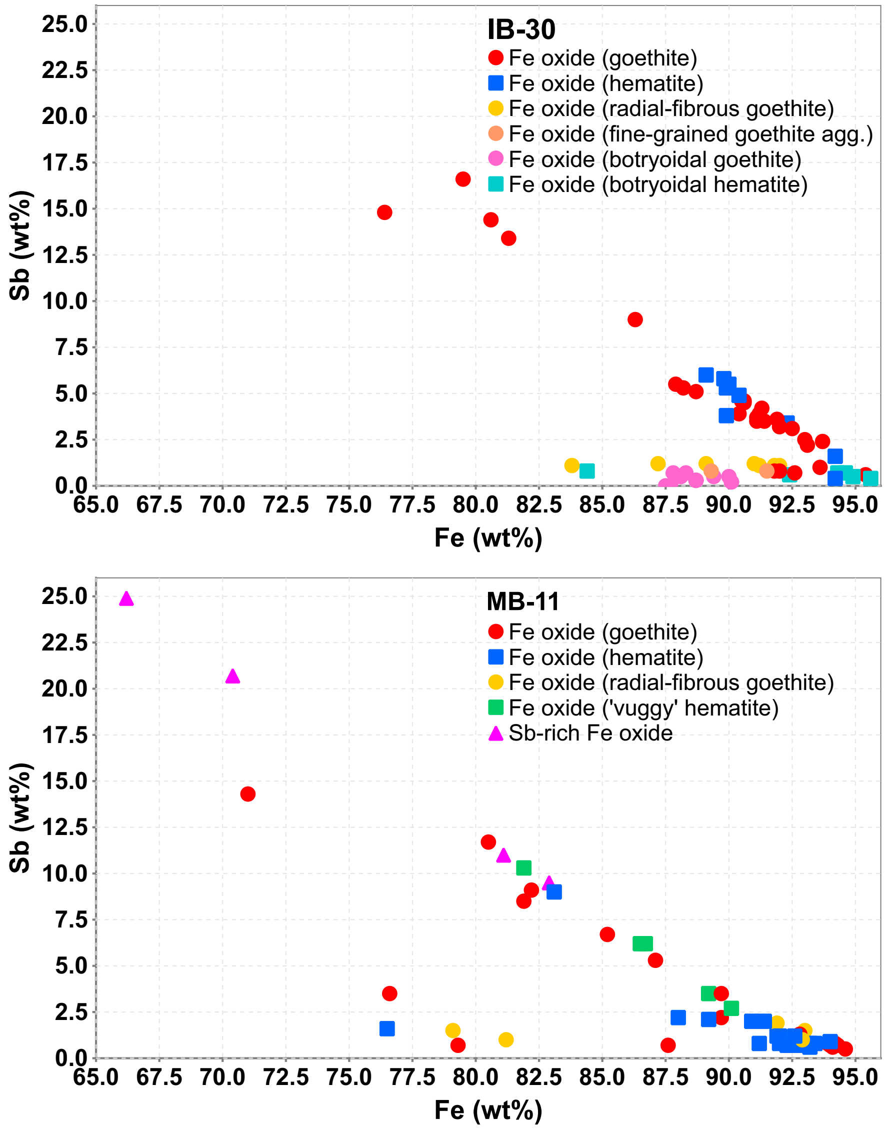

Figure 6. Fe (wt%) vs Sb (wt%) plot for EDS results obtained for samples IB-30 and MB-11.

Table 2. Summary statistics of EDS results for iron oxide from sample MB-11.

Phase	Fe (wt%)	Sb (wt%)	Pb (wt%)	As (wt%)	Zn (wt%)
Fe oxide (goethite) (n = 18)					
min	71.0	0.5	1.5	0.0	0.0
max	94.6	14.3	9.8	2.3	0.7
average	87.2	4.0	3.0	0.8	0.4
median	88.7	1.8	2.6	0.7	0.3
Fe oxide (hematite) (n = 20)					
min	76.5	0.6	3.0	0.3	0.0
max	94.0	9.0	5.7	1.1	0.5
average	90.8	1.5	4.2	0.9	0.1
median	92.2	0.9	4.2	0.9	0.0
Fe oxide (radial-fibrous goethite) (n = 5)					
min	79.1	1.0	1.6	0.6	0.2
max	93.0	1.9	2.4	1.0	0.3
average	87.6	1.4	1.9	0.8	0.3
median	91.9	1.5	1.9	0.8	0.3
Fe oxide (‘vuggy’ hematite) (n = 5)					
min	81.9	2.7	2.8	0.9	0.4
max	90.1	10.3	3.4	1.3	0.9
average	86.9	5.8	3.0	1.1	0.6
median	86.7	6.2	2.9	1.0	0.6
Sb-rich Fe oxide (n = 4)					
min	66.2	9.5	3.5	0.7	0.6
max	82.9	24.9	4.0	1.3	1.3
average	75.2	16.5	3.8	1.0	0.9
median	75.8	15.9	3.8	1.1	0.9

antimony and other abundant critical (eg arsenic, bismuth, selenium, and tellurium) and precious metals (eg silver and gold) from their respective host minerals through a mineral processing characterisation program (termed a 'Stream 3' investigation). These techniques may include hydrometallurgical processes, such as leaching and solvent extraction; or pyrometallurgical methods, depending on the mineralogical composition and the specific extraction requirements.

Acknowledgements

Kathleen Cato, Sherrie Palmer and Natasha Winters from SMI/UQ are thanked for their assistance in the project (project management, sample and figure preparation, and report reviewing). Former SMI/UQ staff Dr Thomas Jones and Dr Zhengdong Han are thanked for help sampling. Dr Pablo Farias, Dr Jo Whelan, Dr Cait Stuart and Dorothy Close from NTGS are thanked for project funding and administration. Dr Michael Green and Arvid Buskas from PNX Metals Ltd are thanked for site access and accommodating the UQ project team during sampling. The SMI MLA lab staff, CMM/UQ, QUT and University of Adelaide are acknowledged for their analytical services. Gregory MacDonald (NTGS) is thanked for revising the abstract.

References

Ahmad M and Hollis JA, 2013. Chapter 5 - Pine Creek Orogen: in Ahmad M and Munson TJ (compilers). *'Geology and mineral resources of the Northern Territory'*. *Northern Territory Geological Survey, Special Publication* 5.

Bhowany K, Han Z, Parbhakar-Fox A, Jones TR, Farias PG, Whelan JA, Close D, Thorne JP and Fraser G, 2023. Secondary prospectivity of mine waste in the Pine Creek region: The search for critical metals: in *'Annual Geoscience Exploration Seminar (AGES) Proceedings, Alice Springs, Northern Territory 17–19 April 2023'*. Northern Territory Geological Survey, Darwin, 138–146.

Britt AF and Senior AB, 2021. *Australian Resource Reviews: Antimony 2020.* Geoscience Australia, Canberra. http://dx.doi.org/10.11636/9781922446534

Dold B, 2020. Sourcing of critical elements and industrial minerals from mine waste – The final evolutionary step back to sustainability of humankind? *Journal of Geochemical Exploration* 219, 106638.

Filella M, Belzile N and Chen Y-W, 2002. Antimony in the environment: a review focused on natural waters: I. Occurrence. *Earth-Science Reviews* 57(1–2), 125–176.

Geological Survey of Canada, 2023. *Critical minerals: an opportunity for Canada*. Government of Canada. https://www.canada.ca/en/campaign/critical-minerals-in-canada/critical-minerals-an-opportunity-for-canada.html. [2 February 2024].

Geoscience Australia, 2024. *Critical minerals at Geoscience Australia*. Geoscience Australia. https://www.ga.gov.au/scientific-topics/minerals/critical-minerals. [2 February 2024].

Gomes AS, Bhowany K, Jackson L, Han Z and Parbhakar-Fox A, 2023. Assessment of mine waste secondary prospectivity: Iron Blow and Mount Bonnie, Northern Territory. *Northern Territory Geological Survey, Record* 2023-015.

Lèbre É, Corder GD and Golev A, 2017. Sustainable practices in the management of mining waste: A focus on the mineral resource. *Minerals Engineering* 107, 34–42.

McEwan K and Ralph D, 2002. The I-BO (TM) process and related treatments for mine waste remediation. *WIT Transactions on Ecology and the Environment* 55.

Radková AB, Jamieson HE, Campbell KM and Hudson-Edwards KA, 2023. Antimony in mine wastes: geochemistry, mineralogy, and microbiology. *Economic Geology* 118(3), 621–637.

Raymond OL, Gallagher R, Shaw R, Yeates AN, Doutch HF, Palfreyman WD, Blake DH and Highet L, 2012. *Surface Geology of Australia 1:2.5 million scale dataset 2012 edition.* Geoscience Australia, Canberra. https://pid.geoscience.gov.au/dataset/ga/73140

Schwarz-Schampera U, 2014. Chapter 4 - Antimony: in Gunn G (editor). *'Critical metals handbook'*. Wiley and Sons Ltd, 70–98. https://doi.org/10.1002/9781118755341.ch4

Stuart-Smith PG, Needham RS, Page RW and Wyborn LAI, 1993. Geology and mineral deposits of the Cullen mineral field. *Bureau of Mineral Resources, Australia, Bulletin* 229.

US Geological Survey, 2024. *Mineral commodity summaries 2024.* United States Geological Survey, Virginia. https://doi.org/10.3133/mcs2024 [2 February 2024].

van der Ent A, Parbhakar-Fox A and Erskine PD, 2021. Treasure from trash: Mining critical metals from waste and unconventional sources. *Science of the Total Environment* 758, 143673.

Worden K, Carson C, Scrimgeour I, Lally J and Doyle N, 2008. A revised Palaeoproterozoic chronostratigraphy for the Pine Creek Orogen, northern Australia: Evidence from SHRIMP U–Pb zircon geochronology. *Precambrian Research* 166(1–4), 122–144.

Zhou J, Nyirenda MT, Xie L, Li Y, Zhou B, Zhu Y and Liu H, 2017. Mine waste acidic potential and distribution of antimony and arsenic in waters of the Xikuangshan mine, China. *Applied Geochemistry* 77, 52–61.